Cross-Conjugated Bis(porphryin)s: Synthesis, Electrochemical Behavior, Mixed Valency, and Biradical Dication Formation

David A. Shultz,* Hyoyoung Lee,† R. Krishna Kumar, and Kevin P. Gwaltney

Department of Chemistry, North Carolina State University, Raleigh, North Carolina 27695-8204

Received June 29, 1999

The synthesis and characterization of seven $(Zn^{II})_2$bis(porphyrin) molecules are described. The molecular structures of two bis(porphyrin)s (**6** and **7**) were determined by X-ray diffraction methods. Four of the compounds have their porphyrin moieties attached in a *meta*-fashion to a substituted benzene ring (**1**−**4**), two have porphyrin rings attached in a *gem*-fashion to a carbon−carbon double bond (**6** and **7**), and one bis(porphyrin) (**5**) has a *p*-phenylene coupler. Bis(porphyrin)s **1**, **4**, and **5** contain tetraaryl-type porphyrins, while **2**, **3**, **6**, and **7** contain triarylethynylporphyrins. Except for exciton coupling in the unoxidized species, interaction between porphyrins is greater in the triarylethynyl-type bis(porphyrin)s than in the tetraaryl-type bis(porphyrin)s regardless of the number of bonds through which the interaction propagates. The cyclic voltammetry of the bis(porphyrin)s was examined, and a varying degree of interaction between electrophores within the series was found. Redox splitting was observed for porphyrin ring oxidations of **3**, **6**, and **7**, suggesting interaction between the oxidized porphyrin rings beyond simple electrostatic repulsions. No such redox splitting was observed for any of the tetraaryl-type bis(porphyrin)s (**1**, **4**, and **5**). We conclude that two porphyrin radical cations interact best when (1) the interaction pathway is short ($\Delta E_{1/2}$(**6**/**7**) > $\Delta E_{1/2}$(**2**/**3**)), (2) π-overlap between the electrophore and coupler is maximized (minimal bond torsions: $\Delta E_{1/2}$(**6**/**7**) > $\Delta E_{1/2}$(**4**/**5**)), and (3) the electron demand of the coupler matches that of the spin carrier ($\Delta E_{1/2}$(**3**) > $\Delta E_{1/2}$(**2**)). One-electron oxidized triarylethynyl-type bis(porphyrin)s exhibit spectral features characteristic of mixed-valent compounds. In two cases (**6**$^{\bullet+}$ and **7**$^{\bullet+}$), near-IR bands near 8300 cm^{-1} were observed and are tentatively assigned to intervalence transitions. Singly oxidized tetraaryl-type bis(porphyrin)s exhibit no such near-IR transitions, and electronic absorption spectra recorded during electrochemical oxidations are marked by isosbestic points, suggesting negligible interaction between the two halves of the molecule, consistent with cyclic voltammetric results. Two-electron oxidation of **2**−**7** yields biradical dications whose frozen solution EPR spectra lack fine structure, but exhibit $\Delta m_s = 2$ transitions characteristic of exchange-coupled $S = 1$ states. Oxidation of **1** yields a biradical in which both exchange coupling and dipolar interaction between unpaired electrons are presumably very weak; consequently no $\Delta m_s = 2$ is observed. The results of variable-temperature EPR spectroscopy of **2**$^{2\bullet2+}$−**7**$^{2\bullet2+}$ suggest either a triplet ground state or a singlet−triplet degeneracy. As a consequence of our results, we hypothesize that the exchange interaction, and therefore the singlet−triplet gap, in a biradical di-ion can be adjusted to favor the triplet state by simple substituent effects.

Introduction

Multispin molecular assemblies featuring metalloporphyrins are promising components of molecule-based magnetic materials. Iwamura prepared free-base porphyrins and metalloporphyrins with one to four phenylcarbene groups.[1,2] The phenylcarbenes can be ferromagnetically *or* antiferromagnetically coupled through the tetraphenylporphyrin core. For example, the *syn*-dicarbene (free-base and zinc-metalated) obeyed the Curie law for a quintet ground state, while the *anti*-isomer is a singlet ground state with the quintet 54 cal higher in energy. In addition, the Cu^{II} monocarbene compound showed ferromagnetic coupling between metal and carbene spins, resulting in a quartet ground state. Kamachi has reported verdazyl-substituted porphyrins attached to polymer backbones that exhibit only weak antiferromagnetic interactions.[1,3] Iwamura has also studied the magnetic behavior of pyridine nitroxides coordinated to Cr^{III} tetraphenylporphyrin.[4] Miller and Epstein have been studying Mn^{II}porphyrin−TCNE complexes, many of which order magnetically.[5−17]

* To whom correspondence should be addressed. E-mail: shultz@chemdept.chem.ncsu.edu. Fax: (919) 515-8920. Phone: (919) 515-6972. World Wide Web: http://www2.ncsu.edu/ncsu/chemistry/das.html.

† Current address: Center for Smart Supramolecules (CSS), Pohang University of Science and Technology (POSTECH), San 31 Hyojadong, Pohang 790-784, South Korea.

(1) Iwamura, H. *Adv. Phys. Org. Chem.* **1990**, *26*, 179.
(2) Koga, N.; Iwamura, H. *Nihon Kagaku Kaishi* **1989**, 1456.
(3) Kamachi, M. *Nihon Butsuri Gakkaishi* **1987**, *42*, 351.
(4) Kitano, M.; Koga, N.; Iwamura, H. *J. Chem. Soc., Chem. Commun.* **1994**, 447.
(5) Miller, J. S.; Calabrese, J. C.; McLean, R. S.; Epstein, A. J. *Adv. Mater.* **1992**, *4*, 498.
(6) Böhm, A.; Vazquez, C.; McLean, R.; Calabrese, J.; Kalm, S.; Manson, J.; Epstein, A.; Miller, J. *Inorg. Chem.* **1996**, *35*, 3083.
(7) Brandon, E. J.; Kollmar, C.; Miller, J. S. *J. Am. Chem. Soc.* **1998**, *120*, 1822.
(8) Brandon, E. J.; Arif, A. M.; Burkhart, B. M.; Miller, J. S. *Inorg. Chem.* **1998**, *37*, 2792.
(9) Brinckerhoff, W. B.; Morin, B. G.; Brandon, E. J.; Miller, J. S.; Epstein, A. J. *J. Appl. Phys.* **1996**, *83*, 6974.
(10) Buschmann, W.; Vazquez, C.; Ward, M.; Jones, N.; Miller, J. *Chem. Commun.* **1997**, 409.
(11) Girtu, N. A.; Wynn, C. M.; Sugiura, K.-I.; Miller, J. S.; Epstein, A. J. *Synth. Met.* **1997**, *85*, 1703.

10.1021/jo991046h CCC: $18.00
Published on Web 11/20/1999

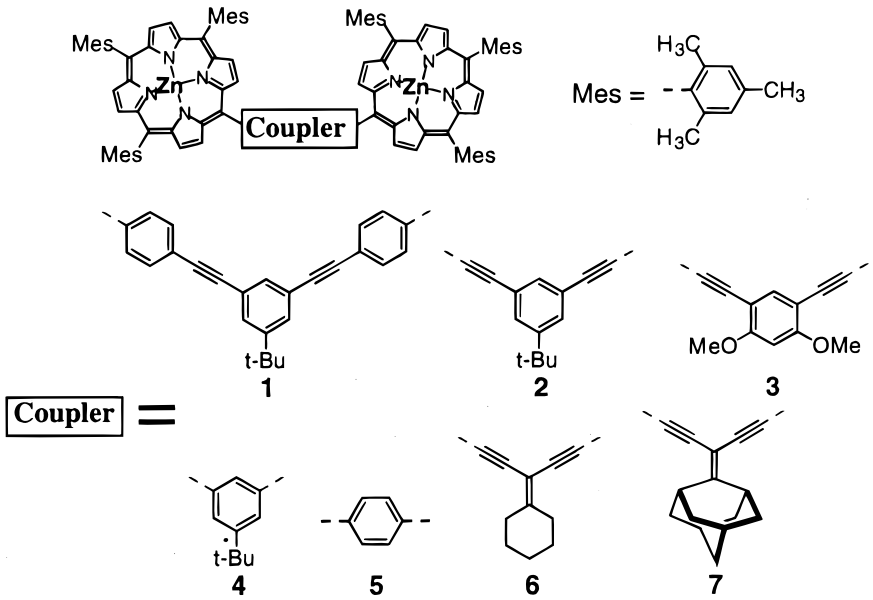

To extend interactions in materials utilizing porphyrins, we have prepared bis(porphyrin)s **1**−**7**. In addition to being useful as building blocks for two- or three-dimensional coordination polymers, the cross-conjugated molecules can be oxidized to yield biradical dications that are exchange coupled by ferromagnetic coupling units.[18,19] Herein, we describe the preparation of several new bis(porphyrin)s, and present EPR spectra that are consistent with exchange coupling in six out of seven of the corresponding biradical dications.

Results

Synthesis. Bis(porphyrin)s **6** and **7** were prepared as described previously,[19,20] while the syntheses of bis(porphyrin)s **1**−**5** are shown below. Phenylacetylene-substituted porphyrin **16** was prepared as described by Lindsey,[21] and coupled to 5-*tert*-butyl-1,3-diiodobenzene, **8**,[22] to give **1** in good yield. 5-Iodo-10,15,20-trimesitylporphyrin, **17**,[23] was coupled to 5-*tert*-butyl-1,3-bis-(2′-trimethylsilanylethynyl)benzene, **9**, and 1,5-dimethoxy-2,4-bis(trimethylsilanylethynyl)benzene, **11**, using our in situ alkyne deprotection protocol[20] to provide bis(porphyrin)s **2** in 68% and **3** in 65% yield, respectively.

Table 1. Summary of Crystal Data, Data Collection, and Refinement Details

	bis(porphyrin) **6**·1.5(C_7H_8)	bis(porphyrin) **7**·4(C_7H_8)
empirical formula	$C_{115.50}H_{105}N_8Zn_2$	$C_{137}H_{128}N_8Zn_2$
fw	1735.81	2017.21
cryst size, mm	0.06 × 0.06 × 0.34	0.08 × 0.12 × 0.18
temp, K	158(2)	158(2)
cryst syst	triclinic	triclinic
space group	$P\bar{1}$	$P\bar{1}$
a, Å	12.9399(2)	13.0929(2)
b, Å	18.3283(3)	19.0849(1)
c, Å	25.4184(3)	25.1560(1)
α, deg	103.937(1)	69.751(1)
β, deg	101.406(1)	78.647(1)
γ, deg	107.230(1)	72.949(1)
V, Å^3	5347.7(1)	5606.23(9)
Z	2	2
μ, mm^{-1}	0.496	0.483
D_{calcd}, g/cm^3	1.078	1.195
F(000)	1828	2132
radiation	Mo Kα	Mo Kα
λ, Å	0.710 73	0.710 73
no. of reflns collected	70 300	70 891
no. of unique reflns	13 974	22 680
no. of params	1144	1182
R	0.1042	0.0851
wR2	0.2919	0.1723
$(\Delta\rho)_{max}$, e/Å^3	0.721	0.871

Gable bis(porphyrin) **4** and *p*-phenylene-linked bis(porphyrin) **5**[24] were prepared by Suzuki couplings[23] of iodide **17** to diboronic esters **13** and **15**,[25] respectively, prepared using the method of Miyaura.[25] The preparations of dibromides **10**[26] and **12**[27] have been reported.

For EPR studies, biradical dications $\mathbf{1}^{2\bullet 2+}$−$\mathbf{7}^{2\bullet 2+}$ were prepared by oxidation of **1**−**7**, respectively, with 2 equiv of tris(4-bromophenyl)amminium hexachloroantimonate.

$$\text{bis(porphyrin)} \xrightarrow[CH_2Cl_2]{\text{2 equiv of } N(4\text{-}BrC_6H_4)_3SbCl_6} [\text{bis(porphyrin)}]^{2\bullet 2+}[SbCl_6^-]_2$$

(12) Epstein, A. J.; Miller, J. S. *Synth. Met.* **1996**, *80*, 231.
(13) *Molecular Magnetism: From Molecular Assemblies to the Devices*; Coronado, E.; Delhaes, P., Gatteschi, D., Miller, J. S., Eds.; Kluwer Academic Publishers: Dordrecht, The Netherlands, 1996; Vol. 321.
(14) Yates, M. L.; Arif, A. M.; Manson, J. L.; Kalm, B. A.; Burkhart, B. M.; Miller, J. S. *Inorg. Chem.* **1998**, *37*, 840.
(15) Wynn, C. M.; Girtu, M. A.; Brinckerhoff, W. B.; Sugiura, K.-I.; Miller, J. S.; Epstein, A. J. *Chem. Mater.* **1997**, *9*, 2156.
(16) Miller, J. S.; Vazquez, C.; Epstein, A. J. *J. Mater. Chem.* **1995**, *5*, 707.
(17) Miller, J. S.; Epstein, A. J. *Angew. Chem., Int. Ed. Engl.* **1994**, *33*, 385.
(18) Shultz, D. A.; Lee, H.; Gwaltney, K. P.; Sandberg, K. A. *Mol. Cryst. Liq. Cryst.* **1999**, *334*, 459.
(19) Shultz, D. A.; Lee, H.; Gwaltney, K. P. *J. Org. Chem.* **1998**, *63*, 7584.
(20) Shultz, D. A.; Gwaltney, K. P.; Lee, H. *J. Org. Chem.* **1998**, *63*, 4034.
(21) Lindsey, J. S.; Prathapan, S.; Johnson, T. E.; Wagner, R. W. *Tetrahedron* **1994**, *50*, 8941.
(22) Sasaki, S.; Iyoda, M. *Chem. Lett.* **1995**, *11*, 1011.
(23) Shultz, D. A.; Gwaltney, K. P.; Lee, H. *J. Org. Chem.* **1998**, *63*, 769.
(24) Yang, S. I.; Lammi, R. K.; Seth, J.; Riggs, J. A.; Arai, T.; Kim, D.; Bocian, D. F.; Holten, D.; Lindsey, J. S. *J. Phys. Chem. B* **1998**, *102*, 9426.
(25) Ishiyama, T.; Murata, M.; Miyaura, N. *J. Org. Chem.* **1995**, *60*, 7508.

Table 2. Selected Geometric Parameters[a] for 6 and 7

geometric param	bis(porphyrin) **6**	bis(porphyrin) **7**	geometric param	bis(porphyrin) **6**	bis(porphyrin) **7**
Zn1···Zn2	11.230	11.314	C96−C97−C100	122.6(9)	123.9(4)
C2···C49	6.250	6.366	C96−C95−C49	177.7(10)	174.4(5)
C2−C99−C98	175.1(10)	177.8(5)	C96−C97−C98	111.8(8)	112.9(3)
C99−C98−C97	170.2(10)	172.5(4)	C98−C97−C100−C105	4.3	3.3
C98−C97−C100	125.4(9)	123.1(4)	C96−C97−C100−C101	3.3	2.4
C97−C96−C95	174.2(9)	172.5(4)	C2···C97···C49	100.92	103.21

[a] Distances in angstroms and bond/dihedral angles in degrees.

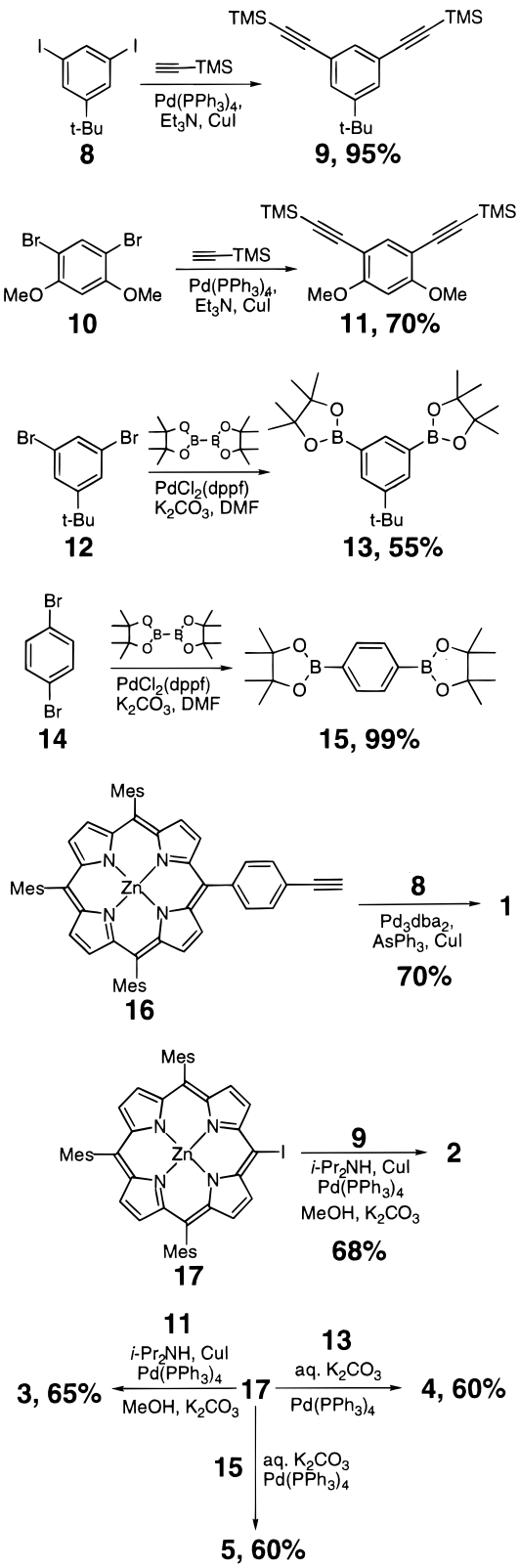

X-ray Crystallography. Crystals of both **6** and **7** were grown by diffusion of pentane into a toluene solution of the bis(porphyrin).[28] ORTEPs of **6** and **7** are shown in Figures 1 and 2, respectively. A summary of the crystallographic data for both **6** and **7** is given in Table 1, and selected geometric parameters are given in Table 2.

Electrochemistry. Bis(porphyrin)s **1**−**7** were examined by cyclic voltammetry (CV), and the results are displayed in Figures 3 and 4, and in Table 3. Only the redox waves associated with the porphyrin/porphyrin$^{\bullet+}$ couples are shown. The two-electron nature of these waves was confirmed by controlled-potential coulometry.

Electronic Absorption Spectroscopy. Electronic absorption spectra of **1**−**7** are shown in Figure 5, and spectroscopic data for these compounds as well as model compound Zn(tetramesitylporphyrin), **ZnTMP**, are collected in Table 4. Bis(porphyrin)s **2**−**7** show split Soret (B) bands, while bis(porphyrin) **1** does not. Numerical values for Soret splitting were determined by fitting the Soret bands to a four-Gaussian model.[28]

Electronic absorption spectra recorded between 20000 cm^{-1} (500 nm) and 7000 cm^{-1} (1429 nm) of **ZnTMP**$^{\bullet+}$, **1**$^{2\bullet2+}$, **4**$^{2\bullet2+}$, and **5**$^{2\bullet2+}$ are shown in Figure 6, while spectra of **2**$^{2\bullet2+}$, **3**$^{2\bullet2+}$, **6**$^{2\bullet2+}$, and **7**$^{2\bullet2+}$ are shown in Figure 7. Pertinent spectroscopic data are collected in Table 4. The spectra in Figures 6 and 7 were collected at various intervals during controlled-potential coulometry. The singly oxidized forms **2**$^{2\bullet+}$, **3**$^{2\bullet+}$, **6**$^{2\bullet+}$, and **7**$^{2\bullet+}$ exhibit unique absorption bands (marked with an asterisk) that are absent in both the un-oxidized forms and the doubly oxidized forms, and are independent of concentration.

EPR Spectroscopy. X-band EPR spectra of **1**$^{2\bullet2+}$−**7**$^{2\bullet2+}$ generated by oxidation with 2 equiv of tris(4-bromophenyl)amminium hexachloroantimonate recorded at 298 K are single, broad lines with unresolved hyperfine structure and a peak-to-peak separation of ca. 7 G. Spectra recorded at 77 K also consist of single lines and thus lack fine structure, but exhibit $\Delta m_s = 2$ transitions characteristic of triplet states, as shown in Figure 8. As noted previously,[19] chemical oxidation of **6** is sometimes accompanied by some decomposition; however, a $\Delta m_s = 2$ transition is observed. The temperature dependence of the doubly integrated $\Delta m_s = 2$ transitions (Curie plots) are shown in Figure 9. Pertinent data are collected in Table 5.

Discussion

Molecular Design Elements. The bis(porphyrin)s presented were prepared for several purposes. For example, we wish to use these molecules for the construction of coordination polymers with interesting magnetic

(26) Kohn, M.; Löff, G. *Monatsh. Chem.* **1924**, *45*, 589.
(27) Ishida, T.; Iwamura, H. *J. Am. Chem. Soc.* **1991**, *113*, 4238.
(28) See the Supporting Information for spectroscopic and crystallographic data.

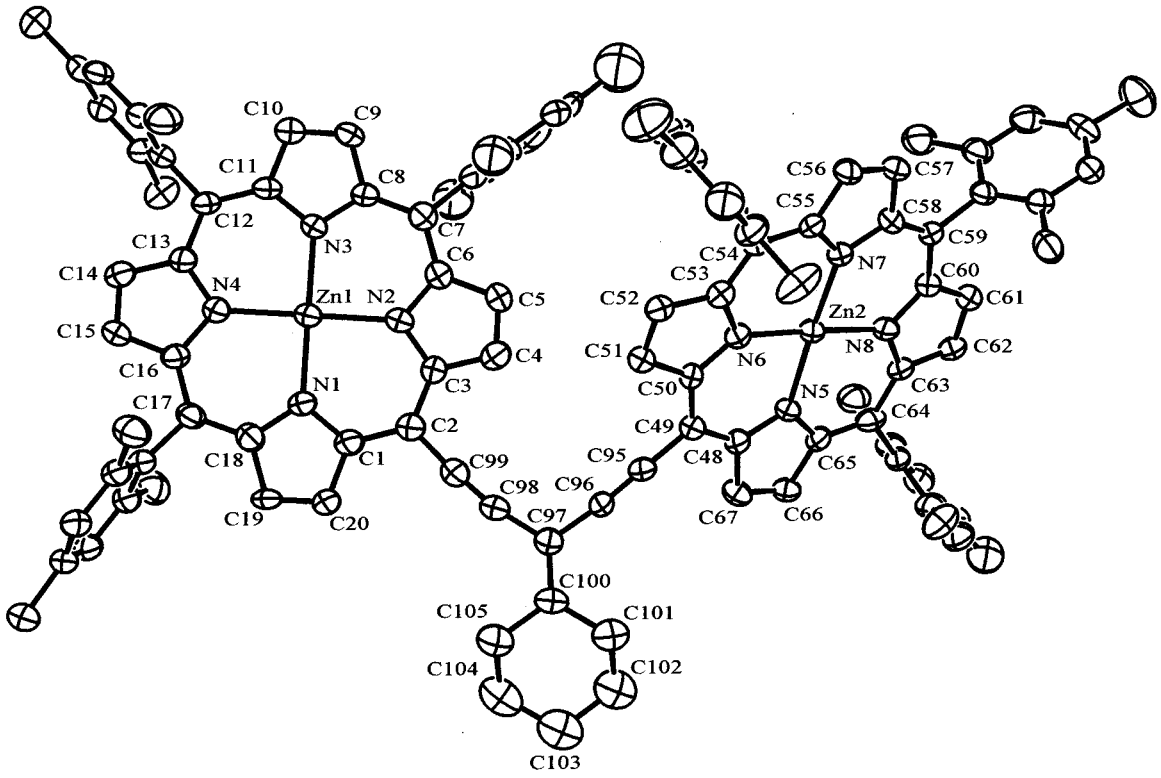

Figure 1. ORTEP of bis(porphyrin) **6**. Hydrogens have been omitted for clarity.

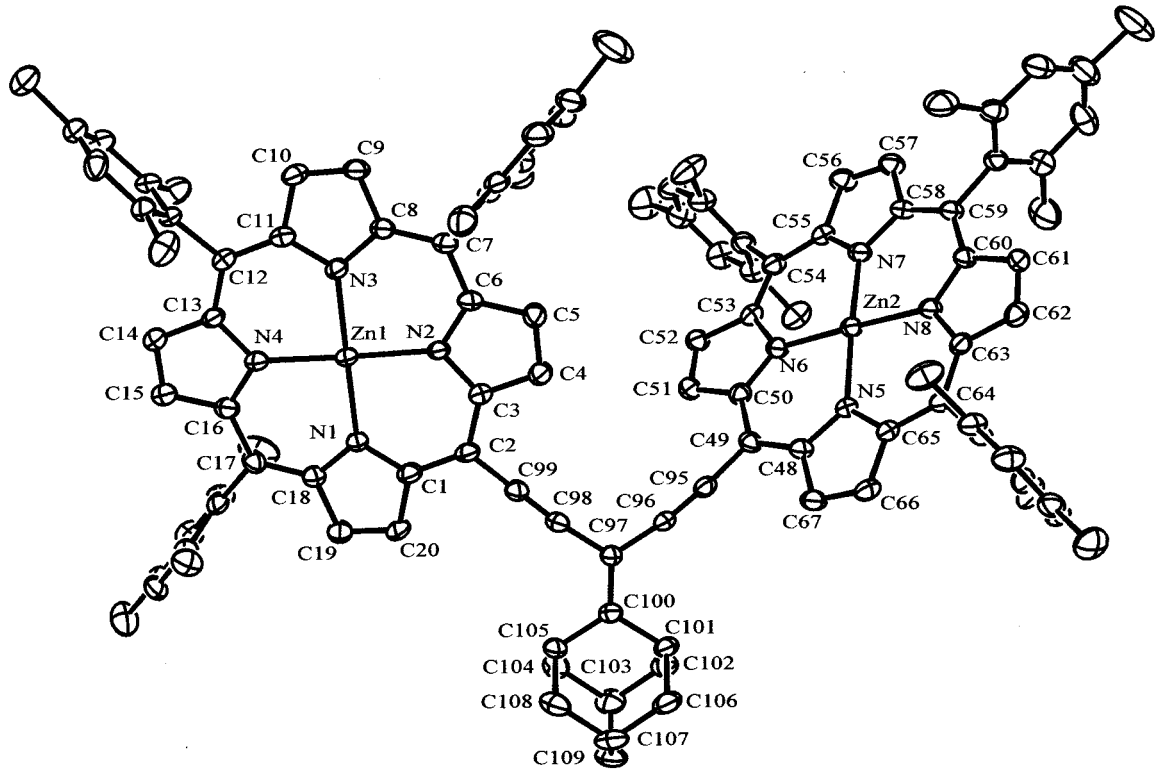

Figure 2. ORTEP of bis(porphyrin) **7**. Hydrogens have been omitted for clarity.

properties, and we are also interested in using porphyrin π radical cations as spin-containing components of high-spin molecules.[18−20,29] Important structural features of **1**−**7** are the mesityl groups. The nearly orthogonal arrangement of mesityl rings with the porphyrin ring[30] reduces the possibility of aggregation, and after oxidation prevents delocalization of spin density into the mesityl groups, thus maximizing spin density in the coupler.

(29) Shultz, D. A.; Sandberg, K. A. *J. Phys. Org. Chem.* **1999**, *12*, 10.

(30) Scheidt, W. R.; Lee, Y. J. In *Structure and Bonding, Vol. 64*; Buchler, J. W., Ed.; Springer-Verlag: Berlin, 1987; pp 1−70.

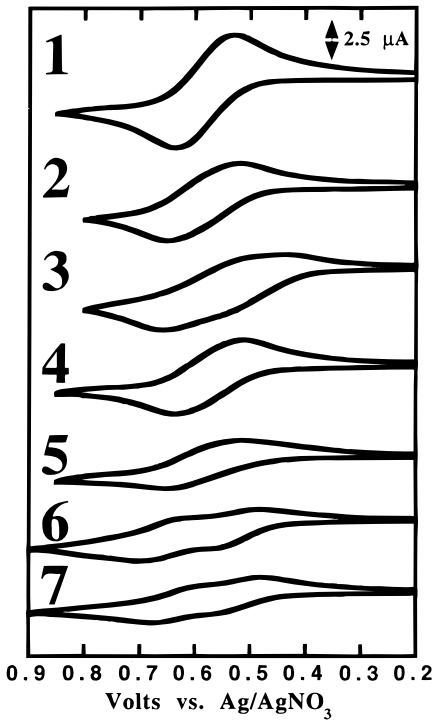

Figure 3. Cyclic voltammograms for **1**−**7** as 1 mM solutions in CH_2Cl_2 (except [**5**] = 0.5 mM). The supporting electrolyte is tetra-*n*-butylammonium hexafluorophosphate (100 mM). Scan rate 100 mV/s.

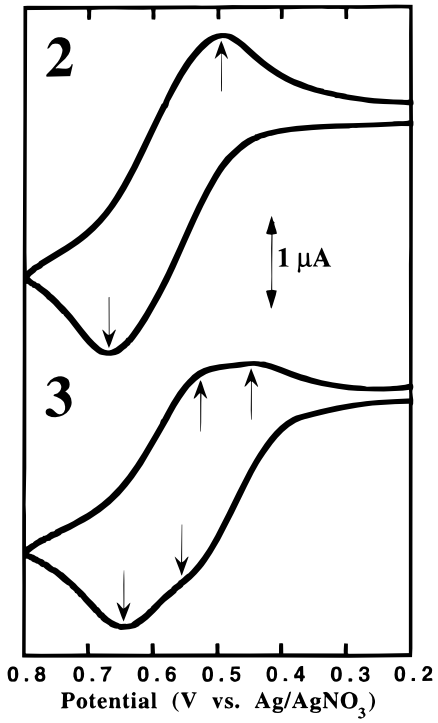

Figure 4. Cyclic voltammograms for **2** and **3** as 1 mM solutions in CH_2Cl_2. The supporting electrolyte is tetra-*n*-butylammonium hexafluorophosphate (100 mM). Scan rate 60 mV/s.

Also, the *meso*-ethynyl groups of **2**, **3**, **6**, and **7** are important for spatially separating the porphyrin rings from the coupler to allow coupler/porphyrin coplanarity necessary for maximal spin−spin coupling in the biradical.

Oxidation of a variety of *meso*-tetraarylmetalloporphyrins gives radical cations having significant spin densities on the *meso*-carbons (SOMOs are a_{2u}-like).[18,29,31−38] To favor intramolecular high-spin coupling of the unpaired electrons of bis(porphyrin) biradical dications, we attached the porphyrins to π-systems (couplers) to give cross-conjugated molecules whose topologies are identical to those of known high-spin organic molecules.[39] That is, $\mathbf{1}^{2\bullet 2+}$−$\mathbf{4}^{2\bullet 2+}$ are *m*-phenylene-type biradicals, and $\mathbf{6}^{2\bullet 2+}$ and $\mathbf{7}^{2\bullet 2+}$ are trimethylenemethane-type (TMM-type) biradicals whose general structures are illustrated below.

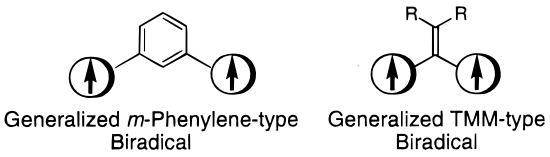

The biradical $\mathbf{5}^{2\bullet 2+}$ serves as a measure of the topology dependence of spin−spin coupling since the unpaired spins should antiferromagnetically couple (below left). Of course, bond torsions between the porphyrin rings and the phenylene coupler will modulate the strength of this interaction. However, spin polarization still predicts antiferromagnetic coupling (below right).[40−42]

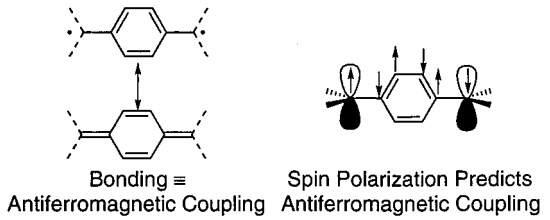

Finally, **3** differs from **2** in that two electron-donating methoxy groups have replaced the *tert*-butyl group of the

(31) Fajer, J.; Borg, D. C.; Forman, A.; Dolphin, D.; Felton, R. H. *J. Am. Chem. Soc.* **1970**, *92*, 3451.
(32) Atamian, M.; Wagner, R. W.; Lindsey, J. L.; Bocian, D. F. *Inorg. Chem.* **1988**, *27*, 1510.
(33) Prendergast, K.; Spiro, T. G. *J. Phys. Chem.* **1991**, *95*, 9728.
(34) Skillman, A. G.; Collins, J. R.; Loew, G. H. *J. Am. Chem. Soc.* **1992**, *114*, 9538.
(35) Song, H.; Reed, C. A.; Scheidt, W. R. *J. Am. Chem. Soc.* **1989**, *111*, 6865.
(36) Erler, B. S.; Scholz, W. F.; Lee, Y. L.; Scheidt, W. R.; Reed, C. A. *J. Am. Chem. Soc.* **1987**, *109*, 2644.
(37) Fujii, H. *Inorg. Chem.* **1993**, *32*, 875.
(38) Fujii, H. *J. Am. Chem. Soc.* **1993**, *115*, 4641.
(39) (a) Shultz, D. A. In *Magnetic Properties of Organic Materials*; Lahti, P., Ed.; Marcel Dekker: New York, 1999. (b) West, A. P., Jr.; Silverman, S. K.; Dougherty, D. A. *J. Am. Chem. Soc.* **1996**, *118*, 1452. (c) Borden, W. T.; Davidson, E. R. *Acc. Chem. Res.* **1996**, *29*, 67. (d) Li, S.; Ma, J.; Jiang, Y. *J. Phys. Chem.* **1996**, *100*, 4775. (e) Rajca, A. *Chem. Rev.* **1994**, *94*, 871. (f) Ichimura, A.; Koga, N.; Iwamura, H. *J. Phys. Org. Chem.* **1994**, *7*, 207. (g) Borden, W. T.; Iwamura, H.; Berson, J. A. *Acc. Chem. Res.* **1994**, *24*, 109. (h) Iwamura, H. *Pure Appl. Chem.* **1993**, *65*, 57. (i) Iwamura, H.; Koga, N. *Acc. Chem. Res.* **1993**, *26*, 346. (j) Dougherty, D. A.; Jacobs, S. J.; Silverman, S. K.; Murray, M.; Shultz, D. A.; West, A. P., Jr.; Clites, J. A. *Mol. Cryst. Liq. Cryst.* **1993**, *232*, 289. (k) Jacobs, S. J.; Shultz, D. A.; Jain, R.; Novak, J.; Dougherty, D. A. *J. Am. Chem. Soc.* **1993**, *115*, 1744. (l) Dougherty, D. A. *Acc. Chem. Res.* **1991**, *24*, 88. (m) Iwamura, H. *Adv. Phys. Org. Chem.* **1990**, *26*, 179. (n) *Kinetics and Spectroscopy of Carbenes and Biradicals*; Platz, M. S., Ed.; Plenum Press: 1990. (o) Iwamura, H. *Pure Appl. Chem.* **1987**, *59*, 1595. (p) Goldberg, A. H.; Dougherty, D. A. *J. Am. Chem. Soc.* **1983**, *105*, 284. (q) Berson, J. A. *Diradicals*; Wiley: New York, 1982. (r) Borden, W. T.; Davidson, E. R. *Acc. Chem. Res.* **1981**, *14*, 69. (s) Borden, W. T.; Davidson, E. R. *J. Am. Chem. Soc.* **1977**, *99*, 4587.
(40) Borden, W. T.; Davidson, E. R. *J. Am. Chem. Soc.* **1977**, *99*, 4587.
(41) Kollmar, H.; Staemmler, V. *Theor. Chim. Acta (Berlin)* **1978**, *48*, 223.
(42) Karafiloglou, P. *J. Chem. Phys.* **1985**, *82*, 3728.

Table 3. Cyclic Voltammetric Data for Bis(porphyrin)s 1−7[a]

bis(porphyrin)	$E_{1/2}$(**1**)[b]	$E_{1/2}$(2)	$\Delta E_{1/2}$[c]	$E_{p,c}$(1)[d]	$E_{p,a}$(1)	$E_{p,c}$(2)	$E_{p,a}$(2)	ΔE_p[e]
1	0.59	0.59	0	0.53	0.64			0.11
2	0.59	0.59	0	0.52	0.65			0.13
3	**0.50**	**0.59**	**0.09**[e]	0.44	0.54[f]	0.53[f]	0.64	0.10, 0.11
4	0.58	0.58	0	0.52	0.64			0.12
5	0.59	0.59	0	0.52	0.65			0.13
6	**0.53**	**0.65**	**0.12**[e]	0.49	0.58[f]	0.60[f]	0.70	0.09, 0.10
7	**0.53**	**0.62**	**0.09**[e]	0.48	0.58[f]	0.57[f]	0.68	0.10, 0.11

[a] 0.1 mM CH_2Cl_2 solution of **1**−**7** (except [**5**] = 0.5 mM) with 100 mM tetra-*n*-butylammonium hexafluorophosphate as supporting electrolyte. Scan rate 120 mV/s. [b] $E_{1/2} = (E_{p,a} - E_{p,c})/2$; potentials in volts vs $Ag/AgNO_3 \pm 20$ mV. [c] Difference between first and second oxidations as determined by the appearance of CV; see the text. [d] Peak potential (c = cathodic, a = anodic). [e] ±20 mV. [f] ±10 mV.

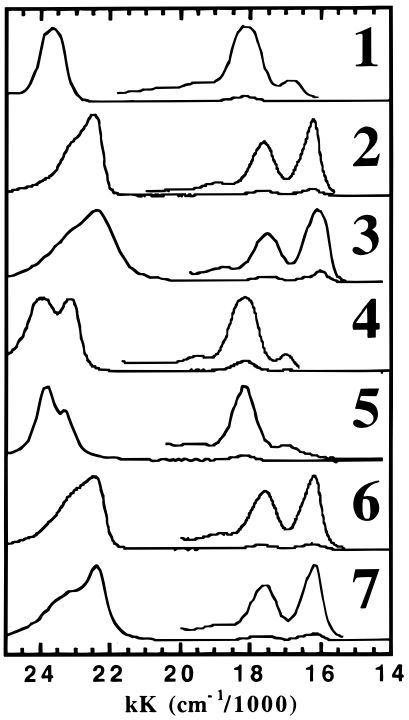

Figure 5. Electronic absorption spectra for bis(porphyrin)s **1**−**7**.

coupler. Thieren has shown that phenyl ring substitution of phenylethynylporphyrins dramatically affects the porphyrin ring oxidation potential.[43] We are particularly interested in modulating spin−spin coupling in biradical di-ions by controlling *electron density* with standard electron-donating or electron-withdrawing groups. This modulation is reasonable since simple MO theory predicts charge and spin are delocalized over the same atoms of a π-radical ion, and therefore spin density might be manipulated by controlling charge density.[44]

The interaction pathway for spin−spin coupling in the cross-conjugated bis(porphyrin) biradical dications *decreases* from $\mathbf{1}^{2\bullet 2+}$ (shortest pathway between porphyrin *meso*-carbons = 16 bonds) to $\mathbf{2}^{2\bullet 2+}/\mathbf{3}^{2\bullet 2+}$ (shortest pathway between porphyrin *meso*-carbons = 8 bonds) to $\mathbf{6}^{2\bullet 2+}/\mathbf{7}^{2\bullet 2+}$ (shortest pathway between porphyrin *meso*-carbons = 6 bonds) to $\mathbf{4}^{2\bullet 2+}$ (shortest pathway between porphyrin *meso*-carbons = 4 bonds), so spin−spin coupling should *increase* in this order. However, it is well-established that *meso*-phenyl substituents in porphyrin radical cations are twisted ca. 40°,[30] so that disruption of porphyrin-coupler conjugation is expected for $\mathbf{1}^{2\bullet 2+}$, $\mathbf{4}^{2\bullet 2+}$, and $\mathbf{5}^{2\bullet 2+}$.[45] Consequently, spin−spin coupling should be attenuated by both bond torsions and distance in $\mathbf{1}^{2\bullet 2+}$ and by bond torsions alone in both $\mathbf{4}^{2\bullet 2+}$ and $\mathbf{5}^{2\bullet 2+}$.[46]

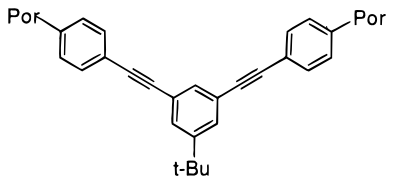

1: shortest coupling through **sixteen** bonds;
$r_{meso\text{-}meso}$ = 16.8 Å

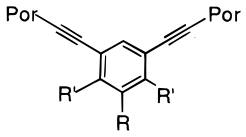

2/3: shortest coupling through **eight** bonds;
$r_{meso\text{-}meso}$ = 9.5 Å

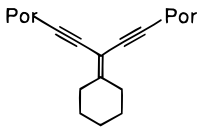

6/7: shortest coupling through **six** bonds;
$r_{meso\text{-}meso} \approx 7.1$ Å

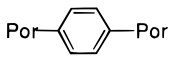

5: shortest coupling through **five** bonds;
$r_{meso\text{-}meso} \approx 5.8$ Å

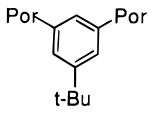

4: shortest coupling through **four** bonds;
$r_{meso\text{-}meso} \approx 5.0$ Å

The crystal structures of both **6** and **7** are made up of discrete molecules of the bis(porphyrin)s. A toluene molecule caps one face of each porphyrin. Thus, the toluene molecules fill the cavities formed by the discrete bis(porphyrin)s. Within the molecules of **6** and **7**, the bond distances and angles are considered normal. The molecular structures of **6** and **7** are quite similar; therefore, only the description of **6** is presented below.

(43) LeCours, S. M.; DiMagno, S. G.; Therien, M. J. *J. Am. Chem. Soc.* **1996**, *118*, 11854.

(44) Computational results corroborate our hypothesis: Shultz, D. A.; Sandberg, K. A.; Dilday, J. S. *J. Phys. Chem.*, to be submitted.

Table 4. UV−Vis Spectroscopic Data for 1−7, Zn^{II}−Tetramesitylporphyrin (ZnTMP), and Biradicals $1^{2•2+}$−$5^{2•2+}$ and $7^{2•2+}$ [a]

bis(porphyrin)	ω_{max}/cm^{-1} (log ϵ)[b]	ω_{max}/cm^{-1} (log ϵ)[c]	bis(porphyrin)	ω_{max}/cm^{-1} (log ϵ)[b]	ω_{max}/cm^{-1} (log ϵ)[c]
1	23 697 (6.03)	20 576 (3.68) 19 455 (3.86) 18 182 (4.66) 16 892 (3.91)	**5**	23 810 (5.44) 23 365 (5.27) [609 cm^{-1}][e]	19 531 (3.63) 18 182 (4.24) 17 007 (3.59)
$\mathbf{1}^{2•2+}$		18 797[d] 15 576 (4.63) 14 948 (4.63) 12 788 (4.60) 11 455 (4.61)	$\mathbf{5}^{2•2+}$		18 182 (4.17) 16 000[d] 14 881 (4.17) 13 089[d] 11 534 (4.13)
2	23 148 (5.72)[d] 22 523 (5.90) [442 cm^{-1}][e]	20 040 (3.69) 18 975 (4.00) 17 668 (4.65) 16 260 (4.79)	**6**	23 095 (5.56)[d] 22 422 (5.77) [502 cm^{-1}][e]	18 868 (4.03) 17 637 (4.55) 16 207 (4.65)
$\mathbf{2}^{2•2+}$		16 181 (4.71) 14 728 (4.73) 13 514 (4.74) 11 587 (4.74) 10 730[d] **11 990**[f]	$\mathbf{6}^{2•2+}$		14 472 (4.56) 12 019 (4.56) **9 671**[d,f] **8 562**[f]
3	23 148 (5.54)[d] 22 422 (5.65) [742 cm^{-1}][e]	18 797 (4.04) 17 544 (4.51) 16 026 (4.92)	**7**	23 148 (5.49)[d] 22 422 (5.67) [591 cm^{-1}][e]	18 868 (3.99) 17 606 (4.50) 16 207 (4.61)
$\mathbf{3}^{2•2+}$		18 868 (4.88) 16 207[d] 14 085 (4.84) 12 870 (4.84) 11 723[d] 10 070 (4.80) **12 300**[f]	$\mathbf{7}^{2•2+}$		11 848 (4.21) 10 142[d] **9 497**[d,f] **8 271**[f]
4	24 038 (5.99) 23 202 (5.94) [824 cm^{-1}][e]	20 747 (3.76) 19 531 (3.97) 18 182 (4.80) 17 007 (4.01)	**ZnTMP**	23 753 (5.70)	19 531 (3.39) 18 182 (4.27) 17 065 (3.31)
$\mathbf{4}^{2•2+}$		19 305 (4.34) 18 018 (4.41) 15 798 (4.57) 14 815 (4.58) 11 628 (4.01)	$\mathbf{ZnTMP}^{•+}$		19 342 (3.56) 17 953 (3.70) 15 773 (3.99) 14 815 (3.95) 11 682 (3.17)

[a] CH_2Cl_2 solutions. [b] Soret region (unoxidized bis(porphyrin)s). [c] Q-band region (unoxidized bis(porphyrin)s). [d] Shoulder. [e] Soret splitting. [f] Tentatively assigned as an intervalence transition: only observed for the singly oxidized, radical cation oxidation state; see the text.

The orientation of the two porphyrin moieties with respect to each other are governed to a major extent by the geometry of the bridging group, especially the ethene coupler. The C96−C97−C98 bond angle of 111.8° is less than the ideal bond angle of 120°. This, along with the distortion of the acetylenic bonds, renders the two porphyrin centers closer than might otherwise be expected. The C2−C97−C49 angle of 100.9° is about 19° less than the ideal value. The porphyrin cores are almost planar: the mean deviation from the least-squares plane including all 25 atoms is 0.029 Å for the porphyrin containing atom Zn1, while it is 0.094 Å for the porphyrin containing atom Zn2. The dihedral angle between the two porphyrin planes is 50.4°. The two porphyrin planes cannot be coplanar due to the overlap of the mesityl groups of both porphyrins.

However, using Chem-3D models of the crystal structures of **6** and **7**, the smallest porphyrin ring torsion angles possible are ca. 25° relative to the Coupler. At smaller dihedral angles, *meso*-mesityl groups attached to different porphyrins are in van der Waals contact. However, both widening of the C96−C97−C98 bond angle to 120° and increasing the alkyne bond angles to 180° allow porphyrin ring torsions of ca. 5° relative to the coupler. Thus, in solution, we believe that the porphyrin rings of both **6** and **7** are able to achieve near coplanarity, and sterics should play a relatively minor role in spin−spin coupling in $\mathbf{2}^{2•2+}/\mathbf{3}^{2•2+}$ and $\mathbf{6}^{2•2+}/\mathbf{7}^{2•2+}$.

Electrochemistry. For **1**, **2**, **4**, and **5** the quasireversible, first oxidation of *each* porphyrin occurs at nearly the same potential. Thus, $E_{1/2}(\mathbf{1})$ and $E_{1/2}(\mathbf{2})$ constitute a single, "two-electron" wave, indicating that interaction between the radical cations is negligible. By the term, "two-electron" wave, we do not mean that $E_{1/2}(\mathbf{1}) = E_{1/2}(\mathbf{2})$, rather that $\Delta E_{1/2}$ is too small to be observed by cyclic

(45) For papers discussing the effects of torsion on exchange coupling, see: (a) Dvolaitzky, M.; Chiarelli, R.; Rassat, A. *Angew. Chem., Int. Ed. Engl.* **1992**, *31*, 180. (b) Kanno, F.; Inoue, K.; Koga, N.; Iwamura, H. *J. Am. Chem. Soc.* **1993**, *115*, 847. (c) Silverman, S. K.; Dougherty, D. A. *J. Phys. Chem.* **1993**, *97*, 13273. (d) Okada, K.; Matsumoto, K.; Oda, M.; Murai, H.; Akiyama, K.; Ikegami, Y. *Tetrahedron Lett.* **1995**, *36*, 6693. (e) Adam, W.; van Barneveld, C.; Bottle, S. E.; Engert, H.; Hanson, G. R.; Harrer, H. M.; Heim, C.; Nau, W. M.; Wang, D. *J. Am. Chem. Soc.* **1996**, *118*, 3974. (f) Fujita, J.; Tanaka, M.; Suemune, H.; Koga, N.; Matsuda, K.; Iwamura, H. *J. Am. Chem. Soc.* **1996**, *118*, 9347. (g) Okada, K.; Imakura, T.; Oda, M.; Murai, H.; Baumgarten, M. *J. Am. Chem. Soc.* **1996**, *118*, 3047. (h) Barone, V.; Bencini, A.; di Matteo, A. *J. Am. Chem. Soc.* **1997**, *119*, 10831. (i) Nakazono, S.; Karasawa, S.; Iwamura, H. *Angew. Chem., Int. Ed. Engl.* **1998**, *37*, 1550. (j) Shultz, D. A.; Boal, A. K.; Lee, H.; Farmer, G. T. *J. Org. Chem.* **1999**, *64*, 4386. (k) Shultz, D. A. In *Magnetic Properties of Organic Materials*; Lahti, P., Ed.; Marcel Dekker: New York, 1999. (l) Ab initio calculations explain antiferromagnetic coupling in *m*-phenylene-linked structures; see: Fang, S.; Lee, M.-S.; Hrovat, D. A.; Borden, W. T. *J. Am. Chem. Soc.* **1995**, *117*, 6727. (m) For several beautiful examples of conformational *J* modulation in metal complexes exchange coupled through organic ligands, see: McCleverty, J. A.; Ward, M. D. *Acc. Chem. Res.* **1998**, *31*, 842.

(46) Sessler reported a gable bis(porphyrin) in which the porphyrin rings were twisted 55° relative to the *m*-phenylene coupler: Sessler, J. L.; Johnson, M. R.; Creager, S. E.; Fettinger, J. C.; Ibers, J. A. *J. Am. Chem. Soc.* **1990**, *112*, 9310.

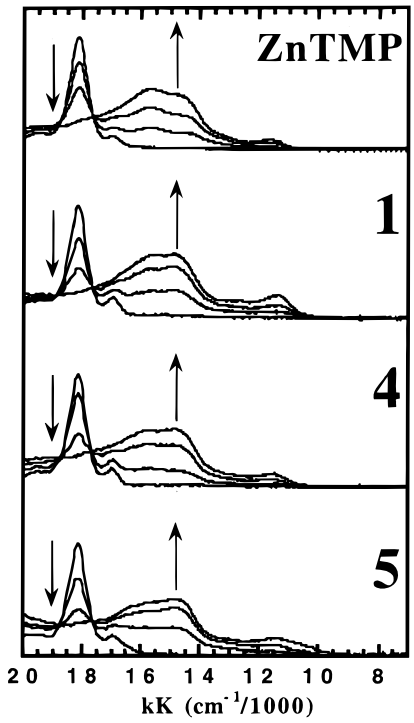

Figure 6. Electronic absorption spectra for model compound **ZnTMP**$^{2\bullet2+}$, and tetraaryl-type bis(porphyrin) biradical dications $\mathbf{1}^{2\bullet2+}$, $\mathbf{4}^{2\bullet2+}$, and $\mathbf{5}^{2\bullet2+}$.

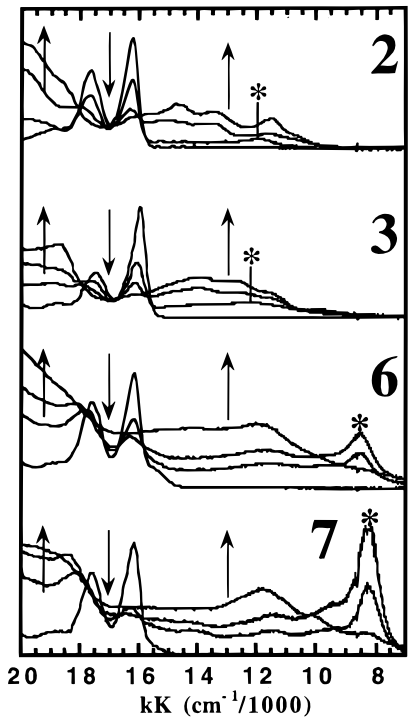

Figure 7. Electronic absorption spectra for triarylethynyl-type bis(porphyrin) biradical dications $\mathbf{2}^{2\bullet2+}$, $\mathbf{3}^{2\bullet2+}$, and $\mathbf{7}^{2\bullet2+}$.

voltammetry. Isolation of the electroactive porphyrin rings is affected by bond torsions of the *meso*-phenyl rings in **1**, **4**, and **5**, as predicted. In bis(porphyrin) **2**, however, no such torsion-induced isolation of the porphyrins exists, and the lack of redox splitting ($E_{1/2}$(**1**) ≈ $E_{1/2}$(**2**)) must be due to weak delocalization through the *meso*-ethynyl group into the *tert*-butyl-*m*-phenylene coupler. In fact, Swager et al. noted minimal redox splitting in ethyne-bridged *p*-phenylenediamines, and concluded that ethyne groups affect *localization* of positive charge, and the observed $\Delta E_{1/2}$ values were attributed solely to electrostatic repulsions.[47]

However, oxidation of the porphyrin rings in **3**, **6**, and **7** occurs at different potentials (split redox waves: $E_{1/2}$(**1**)

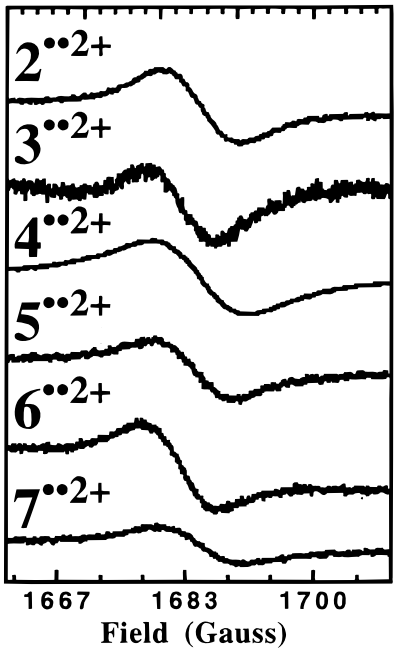

Figure 8. X-band EPR spectra (Δm_s = 2 transitions) of biradical dications $\mathbf{2}^{2\bullet2+}$–$\mathbf{7}^{2\bullet2+}$ recorded at 77 K as solutions in methylene chloride.

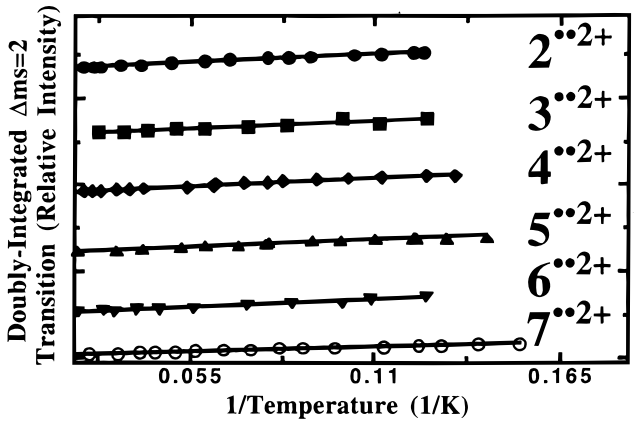

Figure 9. Curie plots (normalized intensities) for biradical dications $\mathbf{2}^{2\bullet2+}$–$\mathbf{7}^{2\bullet2+}$.

Table 5. X-Band EPR Spectroscopy (77 K) Results for Biradicals $\mathbf{1}^{2\bullet2+}$–$\mathbf{7}^{2\bullet2+}$ [a]

biradical	$\Delta m_s = 2$	spectral type	$\lvert D/hc\rvert$ (cm^{-1})
$\mathbf{1}^{2\bullet2+}$	no	double doublet	
$\mathbf{2}^{2\bullet2+}$	yes: $J \geq 0$	biradical	≤0.0007
$\mathbf{3}^{2\bullet2+}$	ues: $J \geq 0$	biradical	≤0.0007
$\mathbf{4}^{2\bullet2+}$	yes: $J \geq 0$	biradical	≤0.0007
$\mathbf{5}^{2\bullet2+}$	yes: $J \geq 0$	biradical	≤0.0007
$\mathbf{6}^{2\bullet2+}$	yes: $J \geq 0$	biradical	≤0.0007
$\mathbf{7}^{2\bullet2+}$	yes: $J \geq 0$	biradical	≤0.0007

[a] Biradical dications prepared by oxidation with 2 equiv of tris-4-bromophenylamminium hexachloroantimonate; [biradical dication] = 10 mM in CH_2Cl_2.

(47) Zhou, Q.; Swager, T. M. *J. Org. Chem.* **1995**, *60*, 7096.

$\neq E_{1/2}$(**2**)), and we contend that the ethynyl groups are efficient at promoting communication beyond simple electrostatic repulsion. Figure 4 shows the cyclic voltammograms of **2** and **3** and better illustrates the difference in redox behavior. Bis(porphyrin)s **2** and **3** are isostructural and differ only in the electron demand of the coupler group. Indeed it is this difference that causes the change from a "two-electron oxidation wave" (**2**) to two, sequential, one-electron waves (**3**). The electron-donating methoxy groups stabilize positive charge by resonance donation, while the *m*-*tert*-butyl is less effective at stabilization. The negative shift in oxidation potentials of **3** compared to **2** (ca. 80 mV) indicates the cation-stabilizing effect of the methoxy groups. Since the methoxy groups of **3** stabilize the radical cation, charge density should increase in and/or near the coupler group and therefore closer to the second porphyrin ring. Thus, interaction of the electrophores (electroactive moieties) in **3** is enhanced relative to **2** and the redox events occur at different potentials. In essence, $\mathbf{3}^{\bullet+}$ represents a class II[48] mixed-valent organic compound,[49−61] and our results parallel quite nicely those of Sutton and Taube for bis(pyridyl)-bridged Ru^{II}/Ru^{III} complexes.[62] Two of their complexes are shown below. Complex **19**, despite the greater number of atoms in the ligand compared to **20**, is a mixed-valence complex where the metal ions interact more strongly than in **20**.

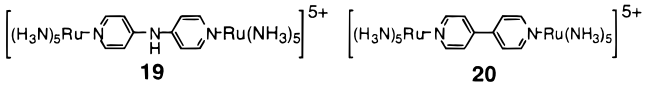

19 **20**

Similar to the results for **2** and **3**, Sutton and Taube observed redox splitting in **19** that was absent in **20**. Both the subtlety and the importance of matching Coupler electron demand with electrophore electron demand is illustrated dramatically in **2**/**3** since both the π-topology and conformation of the couplers are identical and only substituents are different.

$\Delta E_{1/2}$ values similar to those observed here have been attributed to simple electrostatic repulsions;[47,63] however, since no such splitting is observed for redox couples of **4** or **5**, as discussed below, we believe that the origin of the redox splitting in the present case is through-bond.

The fact that electron-donating groups in **3** increase charge delocalization into/toward the coupler implies that spin density is increased in the coupler, and enhanced spin−spin coupling should be observed in biradical dications with electron-rich couplers.[64] We therefore predict that exchange coupling in **3** will be greater than that of **2**. Unfortunately, in the present study we cannot prove this hypothesis. Future work will focus on demonstration of enhancing exchange coupling in biradical di-ions.[44]

Neither gable[65] *m*-phenylenebis(porphyrin) **4** nor *p*-phenylenebis(porphyrin) **5**[24] exhibit redox splitting. This is noteworthy for two reasons. First, despite the fact that the porphyrin units are closer together in cross-conjugated **4** (and electrostatic interaction is greater) than in cross-conjugated **6**/**7**, no redox splitting is observed for **4**. We believe that redox splitting in **6**/**7** is the result of interaction propagated through the π-system, and these compounds in their monooxidized forms, like $\mathbf{3}^{\bullet+}$, are class II mixed-valence molecules.[66] Second, the redox waves for **4** and **5**[24] are indistinguishable. Others[24] and we attribute this to large phenylene bond torsions in both **4** and **5** that insulate each half of the molecule, hence the single redox wave. Again, there are parallels with inorganic species such as those discussed above: torsion between coupler and electrophore results in attenuated $\pi-\pi$ overlap and therefore weak interaction between electrophores.[62,67] Since bond torsions modulate conjugation, the absence of redox splitting in **4**/**5** lends credence to our conclusion that interaction in the biradical dications (and radical cations) is effectively propagated through the ethyne-containing π-system.

To summarize, the two radical cations interact best when (1) the interaction pathway is short ($\Delta E_{1/2}$(**6**/**7**) > $E_{1/2}$(**2**/**3**)), (2) π-overlap between the electrophore and coupler is maximized (minimal bond torsions: $\Delta E_{1/2}$(**6**/**7**) > $E_{1/2}$(**4**/**5**)), and (3) the electron demand of the coupler matches that of the spin carrier ($\Delta E_{1/2}$(**3**) > $E_{1/2}$(**2**)). Point 3 suggests that electron-rich couplers should promote effective interaction of radical cations and electron-poor couplers should promote effective interaction of radical anions.[64] We hypothesize that a necessary consequence of our results is that the exchange interaction (and therefore the singlet−triplet gap) in a biradical di-ion can be adjusted by straightforward substituent effects. We feel also that our hypothesis concerning enhanced exchange coupling when electron demand of the coupler matches those of the charged spin carriers is related to enhanced electron-transfer rates across electron-donor-substituted π-conjugated bridges observed by Wasielewski et al.[68]

Electronic Spectroscopy. Bis(porphyrin)s. The split Soret bands of bis(porphyrin)s **2**−**7** indicate excitonic coupling of the two chromophores, while the lack of

(48) Robin, M. B.; Day, P. *Adv. Inorg. Radiochem.* **1967**, *10*, 247.
(49) Bonvoisin, J.; Launay, J. P.; Rovira, C.; Veciana, J. *Angew. Chem., Int. Ed. Engl.* **1994**, *33*, 2106.
(50) Bonvoisin, J.; Launay, J. P.; Vanderauweraer, M.; DeSchryver, F. C. *J. Phys. Chem.* **1994**, *98*, 5052.
(51) Bonvoisin, J.; Launay, J. P.; Verbouwe, W.; Vanderauweraer, M.; DeSchryver, F. C. *J. Phys. Chem.* **1996**, *100*, 17079.
(52) Coronado, E.; Galan-Mascaros, J. R.; Gimenez-Saiz, C.; Gomez-Garcia, C. J.; Triki, S. *J. Am. Chem. Soc.* **1998**, *120*, 4671.
(53) Domingo, V. M.; Castaner, J. *J. Chem. Soc., Chem. Commun.* **1995**, 895.
(54) Domingo, V. M.; Castañer, J.; Riera, J.; Brillas, E.; Molins, E.; Martinez, B.; Knight, B. *Chem. Mater.* **1997**, *9*, 1620.
(55) Karafiloglou, P.; Launay, J. P. *J. Phys. Chem. A* **1998**, *102*, 8004.
(56) Le Mest, Y.; L'Her, M.; Hendricks, N. H.; Kim, K.; Collman, J. P. *Inorg. Chem.* **1992**, *31*, 835.
(57) Rajca, S.; Rajca, A. *J. Am. Chem. Soc.* **1995**, *117*, 9172.
(58) Sedó, J.; Ruiz, D.; VidalGancedo, J.; Rovira, C. J.; Bonvoisin, J.; Launay, J. P.; Veciana, J. *Adv. Mater.* **1996**, *8*, 748.
(59) Sedó, J.; Ruiz, D.; VidalGancedo, J.; Rovira, C. J.; Bonvoisin, J.; Launay, J. P.; Veciana, J. *Mol. Cryst. Liq. Cryst.* **1997**, *A306*, 125.
(60) Sedó, J.; Ruiz, D.; VidalGancedo, J.; Rovira, C. J.; Bonvoisin, J.; Launay, J. P.; Veciana, J. *Synth. Met.* **1997**, *85*, 1651.
(61) Utamapanya, S.; Rajca, A. *J. Am. Chem. Soc.* **1991**, *113*, 9242.
(62) Sutton, J. E.; Taube, H. *Inorg. Chem.* **1981**, *20*, 3125.
(63) Ferrere, S.; Elliot, C. M. *Inorg. Chem.* **1995**, *34*, 5818 and references therein.
(64) An alternative possibility would be charge−spin separation (for examples of charge−spin separation, see: Niemz, A.; Rotello, V. M. *J. Am. Chem. Soc.* **1997**, *119*, 6833. Wudl, F. *J. Am. Chem. Soc.* **1981**, *103*, 7064). In this case, charge density would increase in the coupler, but spin density would not increase in the coupler. Thus, electron-poor couplers might more strongly couple radical cations. Either way, substituent effects could modulate exchange coupling.
(65) Tabushi, I.; Sasaki, T. *Tetrahedron Lett.* **1982**, *23*, 1913.
(66) We do not mean to imply that $\mathbf{1}^{\bullet+}$, $\mathbf{2}^{\bullet+}$, $\mathbf{4}^{\bullet+}$, and $\mathbf{5}^{\bullet+}$ are not mixed valence (the IT band could be in the IR region), but rather that delocalization in $\mathbf{3}^{\bullet+}$, $\mathbf{6}^{\bullet+}$, and $\mathbf{7}^{\bullet+}$ is greater.
(67) Ward, M. D. *Chem. Soc. Rev.* **1995**, 121.
(68) Davis, W. B.; Svec, W. A.; Ratner, M. A.; Wasielewski, M. R. *Nature* **1998**, *396*, 60.

splitting in **1** suggests that the porphyrin chromophores are sufficiently separated so as to preclude exciton coupling. Interestingly, bis(porphyrin) **1**—which *lacks* Soret splitting—also does *not* exhibit a $\Delta m_s = 2$ transition when doubly oxidized (see below).

The exciton splitting of the Soret band of gable bis(porphyrin) **4** (824 cm^{-1}) is larger than exciton splitting in both the phenylene- (**2** and **5**, but not **3**) and TMM-coupled molecules (**6**, but not **7**), which in turn is greater than that in **1**, which lacks measurable splitting. This variation in exciton splitting is the expected order for an interaction between chromophores that is modulated primarily by interchromophore distance and contrasts nicely the variation in redox behavior that is modulated primarily through π-bonds. The exceptions (**3** and **7**) indicate an additional interaction that is not a function of distance alone.

Electronic Spectroscopy. Oxidized Bis(porphyrin)s. Electronic absorption spectra of $\mathbf{1}^{2\bullet 2+}$—$\mathbf{7}^{2\bullet 2+}$ recorded after controlled-potential coulometry at ca. 0.7 V vs $Ag/AgNO_3$ are shown in Figures 6 and 7 and are characteristic of porphyrin cation radicals: Soret bands that are hypochromically and bathochromically shifted (not shown), and multiple transitions in the visible and near-infrared (near-IR) regions.[69] The triarylethynylporphyrin biradical dications $\mathbf{2}^{2\bullet 2+}$, $\mathbf{3}^{2\bullet 2+}$, $\mathbf{6}^{2\bullet 2+}$, and $\mathbf{7}^{2\bullet 2+}$ exhibit near-IR bands considerably more intense and red-shifted than their oxidized tetraarylporphyrin counterparts.

The bulk electrolyses of the tetraaryl-type bis(porphyrin)s **1**, **4**, and **5** result in absorption spectra that are nearly identical to those of **ZnTMP**, and are marked by isosbestic points (Figure 6). Both of these observations are consistent with negligible interaction between the two halves of the oxidized molecules.

As seen in Figure 7, the singly oxidized forms $\mathbf{2}^{\bullet +}$, $\mathbf{3}^{\bullet +}$, $\mathbf{6}^{\bullet +}$, and $\mathbf{7}^{\bullet +}$ (recorded midway through the bulk electrolysis) exhibit unique electronic absorption bands (marked by an asterisk) characteristic of class II mixed-valent compounds,[48] and are shifted compared to those of Scheidt's mixed-valent [Zn^{II}octaethylporphyrin/Zn^{II}octaethylporphyrin$^{2\bullet +}$] dimers.[70] Since the unique transitions for $\mathbf{2}^{\bullet +}$ and $\mathbf{3}^{\bullet +}$ are obscured by other transitions, we will focus on the near-IR transitions for $\mathbf{6}^{\bullet +}$ and $\mathbf{7}^{\bullet +}$ that appear near 8300 cm^{-1}. The near-IR transitions for $\mathbf{6}^{\bullet +}$/$\mathbf{7}^{\bullet +}$ can also be observed when exhaustive oxidation at 0.7 V vs $Ag/AgNO_3$ is followed by dilution with an equimolar amount of unoxidized **6**/**7**. Thus, comproportionation slightly favors the mixed-valent state, and K_{com} is estimated to be ca. 72 for the equilibrium[71]

$$\mathbf{7} + \mathbf{7}^{2\bullet 2+} \overset{K_{com}}{\rightleftharpoons} 2\ \mathbf{7}^{2\bullet +}$$

From the transition energy, apparent extinction coefficient, and spectral width of the intervalence transitions (IT), barrier heights and mixing coefficients can be calculated using well-known relations.[72] However, the IT bands are far narrower than predicted by Hush's treatment: $\Delta\bar{\omega}_{1/2}(\text{calcd}) \approx 4400\ cm^{-1}$; $\Delta\bar{\omega}_{1/2}(\text{exptl}) \approx 700\ cm^{-1}$. In addition, an additional absorption band exists in the mixed-valent forms appearing as shoulders near 9600 cm^{-1}. These spectral features could be caused by the fact that normal modes involved in intramolecular electron transfer in $\mathbf{6}^{\bullet +}$/$\mathbf{7}^{\bullet +}$ are of greater frequency than the corresponding metal-centered modes of inorganic metal complexes.[73] Thus, in the present case, Hush's equations might not apply. However, a number of organic mixed-valent compounds are known to exhibit Hush-regime IT bands.[49−55,57−61] In addition, the special pair radical cations of the photosynthetic reaction center exhibit unique near-IR bands, one of which is near 8000 cm^{-1} (1200 nm).[74−84] Perhaps $\mathbf{6}^{\bullet +}$/$\mathbf{7}^{\bullet +}$ are uniquely suited as model compounds for studying the special-pair radical cations of the photosynthetic reaction center. In any case, additional spectroscopic studies are warranted to clearly understand the nature of the near-IR transitions of $\mathbf{6}^{\bullet +}$/$\mathbf{7}^{\bullet +}$, and efforts along these lines are underway.

EPR Spectroscopy. None of the biradicals exhibited fine-structure, precluding estimation of the zero-field-splitting parameters, $|D/hc|$, from positions of $\Delta m_s = 1$ transitions and suggesting that the dipole−dipole interactions between unpaired electrons in the biradicals are weak. Collman and co-workers described several cofacial bis(porphyrin) biradicals, only one of which showed zero-field splitting.[56] This 1,8-anthracene-linked bis(porphyrin) biradical had $|D/hc| \approx 0.0047\ cm^{-1}$ (~50 G) despite a ca. 5 Å interporphyrin separation and cofacial alignment.[56,85] A point-dipole estimate[86] of $|D/hc|$ with $r = 5$ Å gives $|D/hc| = 0.021\ cm^{-1}$ (225 G) much greater than Collman's observed D value. Thus, we might expect small zero-field-splitting parameters for our biradical dications.

However, clearly visible near half-field are $\Delta m_s = 2$ transitions, the signature transition of a triplet state, confirming spin−spin coupling in biradicals $\mathbf{2}^{2\bullet 2+}$—$\mathbf{7}^{2\bullet 2+}$, as shown in Figure 8. Notably, $\mathbf{1}^{2\bullet 2+}$ does not exhibit a $\Delta m_s = 2$ transition, indicating that dipolar coupling is negligible, and mirroring the lack of excited-state interaction in unoxidized **1** suggested by the lack of splitting of the Soret band.

The appearance of $\Delta m_s = 2$ transitions for $\mathbf{2}^{2\bullet 2+}$—$\mathbf{7}^{2\bullet 2+}$ permits estimation of D values from the relative intensities of the $\Delta m_s = 1$ and $\Delta m_s = 2$ transitions.[87] These calculations give upper limits of 0.0013 cm^{-1} (14 G) for $|D/hc$ for $\mathbf{2}^{2\bullet 2+}$, $\mathbf{3}^{2\bullet 2+}$, and $\mathbf{7}^{2\bullet 2+}$. Clearly, the calculated D

(69) *The Porphyrins*; Dolphin, D., Ed.; Academic Press: New York, 1978; Vols. 1−7.
(70) Brancato-Buentello, K. E.; Kang, S.-J.; Scheidt, W. R. *J. Am. Chem. Soc.* **1997**, *119*, 2839.
(71) Calculated from $K_{com} = \exp(n_1 n_2 F \Delta E_{1/2}/RT)\}$.
(72) Hush, N. S. *Prog. Inorg. Chem.* **1967**, *8*, 301.
(73) Haberkorn, R.; Michelbeyerle, M. E.; Marcus, R. A. *Proc. Natl. Acad. Sci. U.S.A.* **1979**, *76*, 4185.
(74) Binstead, R. A.; Hush, N. S. *J. Phys. Chem.* **1993**, *97*, 13172.
(75) Breton, J.; Nabedryk, E.; Parson, W. W. *Biochemistry* **1992**, *31*, 7503.
(76) Gasyna, Z.; Schatz, P. N. *J. Phys. Chem.* **1996**, *100*, 1445.
(77) Lendzian, F.; Huber, M.; Isaacson, R. A.; Endeward, B.; Plato, M.; Bonigk, B.; Mobius, K.; Lubitz, W.; Feher, G. *Biochim. Biophys. Acta* **1993**, *1183*, 139.
(78) Osuka, A.; Maruyama, K. *Chem. Lett.* **1987**, 825.
(79) Reimers, J. R.; Hush, N. S. *Inorg. Chim. Acta* **1994**, *226*, 33.
(80) Reimers, J. R.; Hush, N. S. *Chem. Phys.* **1995**, *197*, 323.
(81) Reimers, J. R.; Hutter, M. C.; Hush, N. S. *Photosynth. Res.* **1998**, *55*, 163.
(82) Scheidt, W. R.; Cheng, B. S.; Haller, K. J.; Mislankar, A.; Rae, A. D.; Reddy, K. V.; Song, H. S.; Orosz, R. D.; Reed, C. A.; Cukiernik, F.; Marchon, J. C. *J. Am. Chem. Soc.* **1993**, *115*, 1181.
(83) Stocker, J. W.; Hug, S.; Boxer, S. G. *Biochim. Biophys. Acta* **1993**, *1144*, 325.
(84) Wynne, K.; Haran, G.; Reid, G. D.; Moser, C. C.; Dutton, P. L.; Hochstrasser, R. M. *J. Phys. Chem.* **1996**, *100*, 5140.
(85) Collman's cofacial bis(porphyrin) biradicals (ref 56) have β-octaethyl substitution, and the SOMOs are most likely a_{1u}-like. However, this should alter neither the fact that the two unpaired electrons are delocalized in porphyrin planes that are ca. 5 Å apart, nor the validity of the D-value estimate.
(86) Keana, J. F.; Dinerstein, R. J. *J. Am. Chem. Soc.* **1971**, *93*, 2808.
(87) Weissman, S. I.; Kothe, G. *J. Am. Chem. Soc.* **1975**, *97*, 2537.

values are clearly an overestimation as fine structure should be evident for $|D/hc| = 0.0013$ cm^{-1}. Simulations show that D values of 0.0007 cm^{-1} (7 G), comparable to the spectral line width in frozen solution, lacks fine structure in the $\Delta m_s = 1$ region. The interelectronic distances, ca. 12 Å, estimated from the D value[86] are close to the interporphyrin ring separations (*meso*-carbon to *meso*-carbon distances, ca. 7−10 Å), estimated from molecular models.

The lack of visible fine structure for $\mathbf{4}^{2\bullet 2+}$ and $\mathbf{5}^{2\bullet 2+}$ is somewhat surprising since the point dipole model suggests that the D values for these biradicals should be ca. 8 times the D value for $\mathbf{2}^{2\bullet 2+}$. Perhaps the biradicals in this study serve as examples where the point dipole approximation is inaccurate or perhaps invalid as alluded to above.[88]

The variation of EPR signal intensity as a function of temperature (a Curie plot)[89] can sometimes be used to evaluate the interaction of unpaired electrons. The Curie plots for $\mathbf{2}^{2\bullet 2+}$ and $\mathbf{4}^{2\bullet 2+}$−$\mathbf{7}^{2\bullet 2+}$ shown in Figure 9 are all linear within experimental error. In such cases one can only state that the exchange coupling constant, J ($2J$ = singlet−triplet gap), is consistent with both ferromagnetic coupling ($J > 0$) *and* a singlet−triplet degeneracy ($J = 0$). Ferromagnetic coupling is expected for cross-conjugated, planar biradical dications ($\mathbf{2}^{2\bullet 2+}$, $\mathbf{3}^{2\bullet 2+}$, $\mathbf{6}^{2\bullet 2+}$, and $\mathbf{7}^{2\bullet 2+}$). However, negligible or even antiferromagnetic J might be expected for biradical dications in which considerable torsion between the spin-containing porphyrin radical cations and the phenylene couplers ($\mathbf{4}^{2\bullet 2+}$, $\mathbf{5}^{2\bullet 2+}$) exists.[45] That linear Curie plots are observed for both $\mathbf{4}^{2\bullet 2+}$ *and* $\mathbf{5}^{2\bullet 2+}$ indicates that either the *meso*-carbon spin densities ($\rho \approx 0.16$)[31,32] are insufficient for substantive exchange coupling ($J \approx \rho_i \cdot \rho_j$)[90,91] or bond torsions attenuate the coupling, and the spin polarization mechanism is too weak to affect measurable coupling by the EPR method. We believe the latter to be true since spin densities of ca. 0.16 are large enough to result in measurable exchange coupling.[92−95] However, there are examples in the literature where spin-containing units appear to prefer no coupling ($J = 0$) over antiferromagnetic coupling.[96,97] Additional experimentation is necessary to fully evaluate the exchange coupling in the biradical dications presented here, and efforts along these lines are underway.

Conclusions

The synthesis and characterization of seven $(Zn^{II})_2$bis(porphyrin) molecules were described. Bis(porphyrin)s **1**, **4**, and **5** contain tetraaryl-type porphyrins, while **2**, **3**, **6**, and **7** contain triarylethynylporphyrins. Except for exciton coupling in the unoxidized species, interaction between porphyrins is greater in the triarylethynyl-type bis(porphyrin)s than in the tetraaryl-type bis(porphyrin)s regardless of the number of bonds through which the interaction propagates. The electronic absorption spectra of **2**−**7** exhibit Soret splitting characteristic of interacting chromophores, while the spectrum of **1** exhibits no Soret splitting.

The cyclic voltammetry of the bis(porphyrin)s was examined, and a varying degree of interaction between electrophores within the series was found. Redox splitting was observed for **3**, **6**, and **7**, suggesting interaction between the electroactive porphyrin rings beyond simple electrostatic repulsions. No redox splitting was observed for any of the tetraaryl-type bis(porphyrin)s **1**, **4**, and **5**. It is concluded that two porphyrin radical cations interact best when (1) the interaction pathway is short ($\Delta E_{1/2}$(**6**/**7**) > $E_{1/2}$(**2**/**3**)), (2) π-overlap between the electrophore and coupler is maximized (minimal bond torsions: $\Delta E_{1/2}$(**6**/**7**) > $E_{1/2}$(**4**/**5**)), and (3) the electron demand of the coupler matches that of the spin carrier ($\Delta E_{1/2}$(**3**) > $E_{1/2}$(**2**)).

One-electron-oxidized triarylethynyl-type bis(porphyrin)s exhibit spectral features characteristic of mixed-valent compounds. In two cases ($\mathbf{6}^{\bullet +}$ and $\mathbf{7}^{\bullet +}$), near-IR bands near 8300 cm^{-1} were observed and are tentatively assigned to intervalence transitions. Singly oxidized tetraaryl-type bis(porphyrin)s $\mathbf{1}^{\bullet +}$, $\mathbf{4}^{\bullet +}$, and $\mathbf{5}^{\bullet +}$ exhibit no such near-IR transitions, and electronic absorption spectra recorded during electrochemical oxidations are marked by isosbestic points, suggesting negligible interaction between the two halves of the molecule, consistent with cyclic voltammetric results.

Two-electron oxidation of **2**−**7** yields biradical dications whose frozen-solution EPR spectra lack fine structure, but exhibit $\Delta m_s = 2$ transitions characteristic of exchange-coupled $S = 1$ states. Oxidation of **1** yields a biradical in which exchange coupling and dipolar interactions are presumably very weak; consequently no $\Delta m_s = 2$ is observed. The results of variable-temperature EPR spectroscopy of $\mathbf{2}^{2\bullet 2+}$−$\mathbf{7}^{2\bullet 2+}$ suggest triplet ground states and/or singlet−triplet degeneracies. No topological dependence of the Curie plot on coupler topology was observed: both $\mathbf{4}^{2\bullet 2+}$ and $\mathbf{5}^{2\bullet 2+}$ gave linear Curie plots, despite the prediction of a singlet ground state for the latter. We believe this is consistent with bond torsions localizing the spins, precluding effective (measurable) coupling.

As a consequence of our results, we hypothesize that the exchange interaction, and therefore the singlet−triplet gap, in a biradical di-ion can be adjusted to favor the triplet state by simple substituent effects.[64]

Experimental Section

General Procedures. Chemicals were purchased from Aldrich Chemical Co. unless noted otherwise. Diborane pinacol ester was purchased from Frontier Scientific Inc., Logan, CO. Solvent distillations, synthetic procedures, and electrochemistry were carried out under an argon atmosphere. THF was distilled from sodium benzophenone ketyl prior to use. Methylene chloride was distilled from calcium hydride. Electrochemical experiments and EPR spectroscopy were performed as described previously.[98]

(88) An alteration of Keana's relationship (ref 86) is necessary for accurate estimation of interelectronic separation in dinitroxide biradicals. Gleason, W. B.; Barnett, R. E. *J. Am. Chem. Soc.* **1976**, *98*, 2701. Perhaps in the present cases, neither relationship accurately correlates r and $|D/hc|$.

(89) Berson, J. A. *Diradicals*; Wiley: New York, 1982.

(90) Kahn, O. *Molecular Magnetism*; VCH: New York, 1993.

(91) Rajca, A. *Chem. Rev.* **1994**, *94*, 871.

(92) Mitsumori, T.; Inoue, K.; Koga, N.; Iwamura, H. *J. Am. Chem. Soc.* **1995**, *117*, 2467.

(93) Kanno, F.; Inoue, K.; Koga, N.; Iwamura, H. *J. Phys. Chem.* **1993**, *97*, 13267.

(94) Akita, T.; Mazaki, Y.; Kobayashi, D.; Koga, N.; Iwamura, H. *J. Org. Chem.* **1995**, *60*, 2092.

(95) Yoshioka, N.; Lahti, P. M.; Kaneko, T.; Kuzumaki, Y.; Tsuchida, E.; Nishide, H. *J. Org. Chem.* **1994**, *59*, 4272.

(96) Carilla, J.; Juliá, L.; Riera, J.; Brillas, E.; Garrido, J. A.; Labarta, A.; Alcalá, R. *J. Am. Chem. Soc.* **1991**, *113*, 8281.

(97) Silverman, S. K.; Dougherty, D. A. *J. Phys. Chem.* **1993**, *97*, 13273.

(98) Shultz, D. A.; Farmer, G. T. *J. Org. Chem.* **1998**, *63*, 6254.

X-ray Crystallography. Data Collection for Bis(porphyrin)s 6 and 7. A crystal of suitable dimensions was mounted on a standard Siemens SMART CCD-based X-ray diffractometer equipped with a normal focus Mo-target X-ray tube (λ = 0.710 73 Å) operated at 2000 W power (50 kV, 40 mA). The X-ray intensities were measured at 158(2) K. Analysis of the data showed negligible decay during data collection; the data were corrected for absorption using an empirical method (SADABS: Sheldrick, G. M., SHELXTL, Siemens, Madison, WI, 1995). The structure was solved and refined with the Siemens SHELXTL (version 5.10) software package.

Structure Determination for Bis(porphyrin) 6. The structure was solved and refined using the space group $P\bar{1}$ with $Z = 2$ for the formula $C_{115.5}H_{105}N_8Zn_2$, which includes a total of 1.5 toluene solvates disordered over 4 positions. All non-hydrogen atoms, with the exception of the lattice solvates, were refined anisotropically. Hydrogen atoms were placed in idealized positions. The final full-matrix refinement based on F2 converged at R1 = 0.1042 and wR2 = 0.2919 (based on observed data) and R1 = 0.1458 and wR2 = 0.3249 (based on all data); the largest peak/hole in the final difference map was +0.72/−0.54 Å.

Structure Determination for Bis(porphyrin) 7. The structure was solved and refined using the space group $P\bar{1}$ with $Z = 2$ for the formula $C_{137}H_{128}N_8Zn_{132}$, which includes a total of three toluene solvates. Two of these were located on difference Fourier maps. PLATON identified three additional voids, which may presumably contain additional disordered solvent. These voids cumulatively reflect a potential solvent volume of 681.4 Å^3, which represents a total of 12.2% of the lattice volume. The total electron count per cell is 81.9, and introducing this correction resulted in a dramatic improvement in the reported residuals (10.6% for wR2 and 3.8% for R1 based on all data). These voids likely contain an additional toluene solvate, but this is not definitive. The empirical formula, formula weight, density, absorption coefficient, and $F(000)$ should all therefore be treated with caution. All non-hydrogen atoms, with the exception of the lattice solvates were refined anisotropically. Hydrogen atoms were placed in idealized positions. The final full matrix refinement based on F2 converged at R1 = 0.0851 and wR2 = 0.1723 (based on observed data); R1 = 0.1261 and wR2 = 0.1934 (based on all data) and the largest peak/hole in the final difference map was +0.87/−0.58 Å.

1-*tert*-Butyl-3,5-bis(trimethylsilanylethynyl)benzene, 9. A 100 mL Schlenk flask containing **12**[27] (1.02 g, 3.48 mmol), $Pd(PPh_3)_4$ (201 mg, 0.174 mmol), CuI (20 mg, 0.104 mmol), piperidine (1.7 mL, 17.4 mmol), and trimethylsilylacetylene (1.5 mL, 10.4 mmol) in THF (30 mL) was subjected to three freeze−pump−thaw cycles. The tightly sealed reaction flask was heated to reflux for 60 h. The mixture was allowed to cool, and saturated aqueous NH_4Cl was added. The organic layer was dried over Na_2SO_4, the solvent removed in vacuo, and the residue run through a short flash column (SiO_2, CH_2Cl_2), followed by purification by radial chromatography (SiO_2, pentane), giving **9** as a light yellow oil (988 mg, 87%): ^{1}H NMR ($CDCl_3$) δ 7.43 (s, 3H), 1.30 (s, 9H), 0.25 (s, 18H); ^{13}C NMR ($CDCl_3$) δ 151.3, 132.8, 129.2, 122.9, 104.7, 94.1, 34.7, 31.1, 0.01; IR (film) ν_{max} 2144 cm^{-1}. Anal. Calcd for $C_{20}H_{30}Si_2$: C, 73.54; H, 9.25. Found: C, 73.58; H, 9.34.

1,5-Dimethoxy-2,4-bis(trimethylsilanylethynyl)benzene, 11. A 100 mL Schlenk flask containing dibromide **10**[26] (1.0 g, 3.38 mmol), $Pd(PPh_3)_4$ (195 mg, 0.17 mmol), CuI (19.3 mg, 0.10 mmol), and piperidine (1.67 mL, 16.9 mmol) in THF (50 mL) was sparged with argon for 5 min and pump/purged five times. The reaction mixture was heated to reflux. After 15 min, 1 equiv of trimethylsilylacetylene (1.43 mL, 10.14 mmol) was added quickly with argon purging followed by an additional 3 equiv of trimethylsilylacetylene every 5 h thereafter until a total of 12 equiv had been added. After an additional 24 h at reflux, the mixture was allowed to cool, and ether and saturated aqueous NH_4Cl were added. The layers were separated, the organic layer was dried over Na_2SO_4, and the solvent was removed in vacuo. The residue was run through a short flash column (SiO_2, CH_2Cl_2), followed by purification by radial chromatography (SiO_2, 5% CH_2Cl_2/pentane), giving the product as a white solid (782 mg, 70%): ^{1}H NMR ($CDCl_3$) δ 7.52 (s, 1H), 6.32 (s, 1H), 3.88 (s, 6H), 0.23 (s, 18H); ^{13}C NMR ($CDCl_3$) δ 162.0, 139.4, 104.8, 100.3, 97.2, 94.7, 56.0, 0.1; IR (film) ν_{max} 2152 cm^{-1}. Anal. Calcd for $C_{18}H_{26}O_2Si_2$: C, 65.40; H, 7.29. Found: C, 65.22; H, 8.06.

5-*tert*-Butylbenzene-1,3-diboronic Acid Dipinacol Ester, 13. A 25 mL Schlenk flask containing $PdCl_2$(dppf) (50 mg, 0.06 mmol), KOAc (607 mg, 6.16 mmol), diborane pinacol ester (574 mg, 2.26 mmol), and **12**[27] (300 mg, 1.03 mmol) in DMF (11 mL) was prepared in a glovebox. The reaction mixture was heated to 80 °C for 11 h. After cooling, DMF was removed by bulb-to-bulb distillation, and the reaction residue was dissolved in CH_2Cl_2. The residue was passed through a short Celite column and then purified by triethylamine-deactivated silica gel column chromatography (1% triethylamine, 90% CH_2Cl_2/petroleum ether). The resulting product was recrystallized with *n*-pentane and CH_2Cl_2, giving **13** as a white solid (215 mg, 55%): ^{1}H NMR (CD_2Cl_2) δ 7.96 (s, 1H), 7.87 (s, 2H), 1.34 (s, 33H); ^{13}C NMR (CD_2Cl_2) δ 150.1, 139.3, 134.7, 84.3, 35.1, 31.8, 25.3. Anal. Calcd for $C_{22}H_{36}O_4Br_2$: C, 68.43; H, 9.39. Found: C, 68.25; H, 9.38.

Benzene-1,4-diboronic Acid Dipinacol Ester, 15.[25] A 25 mL Schlenk flask containing $PdCl_2$(dppf) (44.6 mg, 0.06 mmol), KOAc (540 mg, 5.46 mmol), diborane pinacol ester (508 mg, 2.0 mmol), and *p*-diiodobenzene (300 mg, 0.91 mmol) in DMF (10 mL) was prepared in a glovebox. The reaction mixture was heated to 80 °C for 19 h. After cooling, DMF was removed by bulb-to-bulb distillation, and the reaction residue was dissolved in CH_2Cl_2 and passed through a short Celite column. Purification was achieved by triethylamine-deactivated silica gel column chromatography (1% triethylamine/petroleum ether). The resulting product was recrystallized with *n*-pentane and CH_2Cl_2, giving **15** as a white solid (232 mg, 99%). This compound was identical to that reported by Ishiyama.[25]

5-*tert*-Butyl-1,3-diphenylethynyl-4′,4″-bis[Zn(II)-trimesitylporphyrinyl]benzene, 1. A 100 mL Schlenk flask containing ethyneporphyrin **16**[21] (141 mg, 0.17 mmol), diiodobenzene **8**[22] (31 mg, 0.8 mmol), toluene (40 mL) and triethylamine (8 mL) was sparged with argon at 35 °C for 30 min. $Pd_2(dba)_3$ (22 mg, 0.02 mmol) and $AsPh_3$ (52 mg, 0.17 mmol) were then added. After the mixture was stirred for 1 h, the solvent was removed in vacuo, and ether and saturated NH_4Cl were added. The layers were separated, and the organic portion was dried over Na_2SO_4, filtered, and evaporated. The residue was subjected to flash chromatography (SiO_2, 1% diethyl ether/petroleum ether) and MPLC (1% diethyl ether/petroleum ether), giving **1** (100 mg, 70%): ^{1}H NMR (CD_2Cl_2) δ 8.92 (d, 4H, J = 4.4 Hz), 8.77 (d, 4H, J = 4.7 Hz), 8.71 (br s, 8H), 8.27 (d, 4H, J = 4.7 Hz), 7.99 (d, 4H, J = 4.7 Hz), 7.79 (br s, 1H), 7.79 (br s, 2H), 7.30 (br s, 12H), 2.62 (br s, 18H), 1.84 (br s, 36H), 1.49 (s, 9H); ^{13}C NMR (CD_2Cl_2) δ 152.7, 150.6, 150.5, 150.4, 150.3, 143.9, 139.7, 139.6, 138.1, 135.2, 132.5, 131.7, 131.6, 131.2, 130.4, 129.7, 128.2, 124.0, 122.8, 119.8, 119.5, 119.5, 90.5, 90.1, 35.4, 31.6, 21.9, 21.8; UV−vis ($CHCl_3$) λ_{max}/nm (log ϵ) 294 (4.81), 402 (4.93), 422 (6.03), 486 (3.68), 514 (3.86), 550 (4.66), 592 (3.91); MS-FAB $C_{120}H_{102}N_8Zn_2$ calcd exact mass 1782.6788, obsd 1782.6810.

3-*tert*-Butyl-1,5-[2′(Zn(II)-trimesitylporphyrinyl)ethynyl]benzene, 2. A 50 mL flask containing iodoporphyrin **17**[23] (233 mg, 0.28 mmol), K_2CO_3 (86 mg, 0.62 mmol), piperidine (0.28 mL, 2.83 mmol), $Pd(PPh_3)_4$ (13.1 mg, 0.01 mmol), CuI (1.1 mg, 0.006 mmol), **9** (86 mg, 0.62 mmol), THF (30 mL), and distilled methanol (3 mL) was pump/purged 10 times, and then refluxed for 16 h. Once cool, ether and saturated NH_4Cl were added. The organic layer was washed two times with saturated NaCl solution, separated, and dried over Na_2SO_4, and the solvent was removed in vacuo. The product was purified by flash chromatography (alumina, 5% CH_2Cl_2/0.1% diethyl ether/petroleum ether to 20% CH_2Cl_2/2% diethyl ether/petroleum ether), giving **2** (124 mg, 68%): ^{1}H NMR (CD_2Cl_2) δ 9.94 (d, 4H, J = 4.4 Hz), 9.40 (d, 4H, J = 4.7 Hz), 8.67 (br s, 8H), 8.59 (br s, 1H), 8.24 (d, 2H, J = 1.5 Hz), 7.35 (s, 8H), 7.30 (s, 4H), 2.66 (s, 12H), 2.63 (s, 6H), 1.90 (s, 24H), 1.88 (s, 12H),

1.66 (s, 9H); ^{13}C NMR (CD_2Cl_2) δ 153.2, 152.8, 151.0, 150.4, 150.2, 139.8, 139.4, 138.3, 132.1, 131.9, 131.7, 131.5, 129.4, 128.3, 125.3, 121.3, 120.6, 99.3, 96.3, 93.5, 35.7, 31.8, 22.0, 21.8; IR (film) ν_{max} 2193 cm^{-1}; UV−vis ($CHCl_3$) λ_{max}/nm (log ϵ) 353 (4.41), 432 (5.72), 444 (5.90), 499 (3.69), 527 (4.00), 566 (4.65), 615 (4.79); MS-FAB $C_{108}H_{94}N_8Zn_2$ calcd exact mass 1630.6183, obsd 1630.6163.

2,4-Dimethoxy-1,5-bis[2′(Zn(II)-trimesitylporphyrinyl)-ethynyl]benzene, 3. A 100 mL Schlenk flask containing **11** (40 mg, 0.12 mmol), iodoporphyrin **17**[23] (216 mg, 0.25 mmol), and K_2CO_3 (74 mg, 0.27 mmol) in THF (20 mL) was sparged with argon for 5 min. Piperidine (0.24 mL, 1.2 mmol), Pd(PPh_3)$_4$ (14 mg, 0.01 mmol), CuI (1.2 mg, 0.003 mmol), and distilled methanol (2.6 mL) were added, and the reaction mixture was pump/purged five times with argon and then refluxed for 36 h. Once cool, the reaction mixture was run through a short flash chromatography column (SiO_2, CH_2Cl_2/THF), and then purified by flash chromatography (SiO_2, 30−50% CH_2Cl_2/petroleum ether), giving **3** (128 mg, 65%): ^{1}H NMR (CD_2Cl_2) δ 9.99 (d, 4H, J = 4.7 Hz), 8.86 (d, 4H, J = 4.7 Hz), 8.64 (s, 8H), 8.58 (s, 1H), 7.33 (d, 12H, J = 14.7 Hz), 6.95 (s, 1H), 4.39 (s, 6H), 2.63 (d, 18H, J = 13.1 Hz), 1.87 (d, 36H, J = 7.3 Hz); ^{13}C NMR (CD_2Cl_2) δ 163.0, 152.4, 150.6, 150.3, 149.9, 139.6, 139.2, 138.1, 136.7, 131.8, 131.6, 131.3, 128.1, 120.6, 120.3, 106.8, 100.5, 96.4, 96.1, 92.6, 57.0, 21.7, 21.6; UV−vis ($CHCl_3$) λ_{max}/nm (log ϵ) 432 (5.54), 446 (5.65), 532 (4.04), 570 (4.51), 624 (4.92); MS-FAB $C_{106}H_{90}N_8O_2Zn_2$ calcd exact mass 1634.58, obsd 1634.58.

3-*tert*-Butyl-1,5-bis[Zn(II)-trimesitylporphyrinyl]benzene, 4. A 25 mL Schlenk flask containing **13** (51 mg, 0.13 mmol), iodoporphyrin **17**[23] (250 mg, 0.29 mmol), Pd(PPh_3)$_4$ (80 mg, 0.007 mmol), and K_3PO_4 (93 mg, 0.44 mmol) in DMF (5 mL) was prepared in a glovebox. The reaction mixture was heated to 100 °C for 12 h. DMF was removed by bulb-to-bulb distillation, and the residue was dissolved in CH_2Cl_2 and poured into a separatory funnel. The ether solution was washed with saturated aqueous NH_4Cl, and the layers were separated. The organic layer was dried over Na_2SO_4 and filtered and the solvent removed in vacuo. The residue was run through a short flash chromatography column (SiO_2, 1% THF/CH_2Cl_2). The solvents were removed, and the residue was dissolved in CH_2Cl_2. After cooling and filtration, the purple solid was purified by radial chromatography (SiO_2, 5−10% CH_2Cl_2/petroleum ether), giving **4** as a purple solid (126 mg, 60%): ^{1}H NMR ($CDCl_3$) δ 9.35 (d, 4H, J = 4.4 Hz), 8.97 (s, 1H), 8.88 (d, 4H, J = 4.4 Hz), 8.71 (s, 8H), 8.63 (s, 2H), 7.32 (s, 4H), 7.27 (s, 8H), 2.65 (s, 12H), 2.63 (s, 6H), 1.93−1.72 (m, 45H); ^{13}C NMR (CD_2Cl_2) δ 150.5, 150.1, 140.8, 139.5, 139.3, 139.2, 137.6, 132.5, 131.3, 131.1, 127.8, 119.1, 118.7, 35.4, 32.1, 22.0, 21.7; UV−vis (CH_2Cl_2) λ_{max}/nm (log ϵ) 307 (4.61), 353 (4.45), 416 (5.99), 431 (5.94), 482 (3.76), 512 (3.97), 550 (4.80), 588 (4.01); MS-FAB $C_{104}H_{94}N_8Zn_2$ calcd exact mass 1582.6184, obsd 1582.6281.

1,4-Bis[Zn(II)-trimesitylporphyrinyl]benzene, 5.[24] A 25 mL Schlenk flask containing **15**[25] (27 mg, 0.11 mmol), **17**[23] (179 mg, 0.21 mmol), Pd(PPh_3)$_4$ (6 mg, 0.007 mmol), and K_3PO_4 (74 mg, 0.35 mmol) in DMF (4 mL) was prepared in a glovebox. The reaction mixture was heated to 100 °C for 24 h. DMF was removed by bulb-to-bulb distillation, and the residue was dissolved in $CHCl_3$. After cooling in the freezer, **5** was filtered off as a purple solid (193 mg, 60%): UV−vis (CH_2Cl_2) λ_{max}/nm (log ϵ) 294 (4.81), 402 (4.93), 422 (6.03), 486 (3.68), 514 (3.86), 550 (4.66), 592 (3.91); MS-FAB $C_{100}H_{86}N_8Zn_2$ calcd exact mass 1526.5558, obsd 1526.5505.

Acknowledgment. This work was funded by the National Science Foundation (Grant CHE-9501085) under the CAREER Program, and by Research Corp. (Grant CS0127) under the Cottrell Scholars Program. D.A.S. also thanks the Camille and Henry Dreyfus Foundation for a Camille Dreyfus Teacher-Scholar Award. Mass spectra were obtained at the Mass Spectrometry Laboratory for Biotechnology. Partial funding for the Facility was obtained from the North Carolina Biotechnology Center and the National Science Foundation. The MALDI-TOF mass spectrometer was funded in part by the North Carolina Biotechnology Center. We thank Dr. Jeff Kampf (Department of Chemistry, University of Michigan) for determining the crystal structures of **6** and **7**, and Professor Stefan Franzen (Department of Chemistry, North Carolina State University) for stimulating discussions and fitting Soret bands.

Supporting Information Available: Spectral and crystallographic data. This material is available free of charge via the Internet at http://pubs.acs.org.

JO991046H